Conference paper

Kirill V. Kovtunov, Oleg G. Salnikov, Ivan V. Skovpin, Nikita V. Chukanov, Dudari B. Burueva and Igor V. Koptyug*

Catalytic hydrogenation with parahydrogen: a bridge from homogeneous to heterogeneous catalysis

https://doi.org/10.1515/pac-2020-0203

Abstract: One of the essential themes in modern catalysis is that of bridging the gap between its homogeneous and heterogeneous counterparts to combine their individual advantages and overcome shortcomings. One more incentive can now be added to the list, namely the ability of transition metal complexes to provide strong nuclear magnetic resonance (NMR) signal enhancement upon their use in homogeneous hydrogenations of unsaturated compounds with parahydrogen in solution. The addition of both H atoms of a parahydrogen molecule to the same substrate, a prerequisite for such effects, is implemented naturally with metal complexes that operate via the formation of a dihydride intermediate, but not with most heterogeneous catalysts. Despite that, it has been demonstrated in recent years that various types of heterogeneous catalysts are able to perform the required pairwise H_2 addition at least to some extent. This has opened a major gateway for developing highly sensitive and informative tools for mechanistic studies of heterogeneous hydrogenations and other processes involving H_2. Besides, production of catalyst-free fluids with NMR signals enhanced by 3-4 orders of magnitude is essential for modern applications of magnetic resonance imaging (MRI), including biomedical research and practice. The ongoing efforts to design heterogeneous catalysts which can implement the homogeneous (pairwise) hydrogenation mechanism are reported.

Keywords: alkynes; heterogeneous catalysis; hydrogenation; immobilization; Mendeleev-21; NMR; reaction mechanisms.

Introduction

Processes that involve molecular hydrogen (H_2) are widespread in industrial catalysis. For instance, selective hydrogenation of alkynes and dienes in alkene streams is used to produce olefins suitable for catalytic polymerization. Given the scale at which these industrial processes are performed, a detailed understanding of reaction mechanisms involved could be a major asset for the development of cleaner and more efficient chemical industry. NMR is certainly one of the key analytical techniques that is widely used in fundamental catalysis research, which is able to provide useful information on the mechanisms and kinetics of various

Article note: A collection of invited papers based on presentations at 21st Mendeleev Congress on General and Applied Chemistry (Mendeleev-21), held in Saint Petersburg, Russian Federation, 9–13 September 2019.

***Corresponding author: Igor V. Koptyug**, International Tomography Center, SB RAS, Institutskaya St. 3A, Novosibirsk, 630090, Russia; Novosibirsk State University, Pirogova St. 1, Novosibirsk, 630090, Russia; and Boreskov Institute of Catalysis, SB RAS, 5 Acad. Lavrentiev Ave., Novosibirsk, 630090, Russia, e-mail: koptyug@tomo.nsc.ru

Kirill V. Kovtunov, Nikita V. Chukanov and Dudari B. Burueva: International Tomography Center, SB RAS, Institutskaya St. 3A, Novosibirsk, 630090, Russia; Novosibirsk State University, Pirogova St. 1, Novosibirsk, 630090, Russia

Oleg G. Salnikov and Ivan V. Skovpin: International Tomography Center, SB RAS, Institutskaya St. 3A, Novosibirsk, 630090, Russia; Novosibirsk State University, Pirogova St. 1, Novosibirsk, 630090, Russia; and Boreskov Institute of Catalysis, SB RAS, 5 Acad. Lavrentiev Ave., Novosibirsk, 630090, Russia

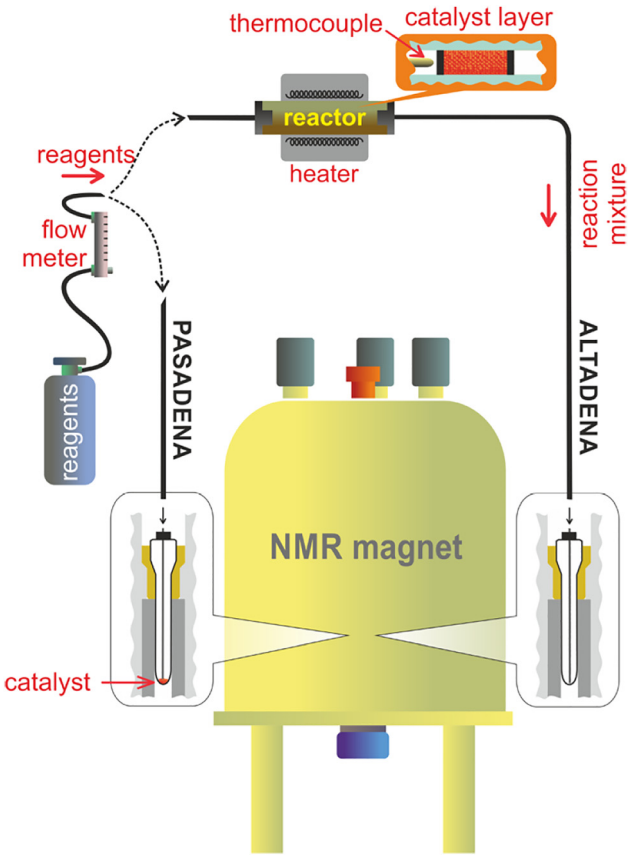

Fig. 1: Schematics of the PHIP experimental setup and protocols. In the PASADENA experiment, the reaction is performed in the high magnetic field of an NMR magnet by supplying gaseous reactants (e. g., propylene and p-H_2) to the solid catalyst placed at the bottom of the NMR tube which resides in the NMR magnet/probe (gas-solid reactions); or by bubbling p-H_2 into the solution of reactant in the presence of a homogeneous or heterogeneous catalyst (gas-liquid and gas-liquid-solid reactions, respectively). In ALTADENA experiments, the reaction is performed in the reactor placed in the low (e. g., Earth's) magnetic field outside the NMR magnet and the reaction mixture is then supplied to the NMR tube residing in the NMR magnet/probe for spectra acquisition. Reprinted with permission from [1]. Copyright 2018 American Chemical Society.

catalytic processes. However, compared to other techniques, NMR is often limited by its relatively low detection sensitivity associated with the weak interaction of nuclear spins with permanent and oscillating magnetic fields that are used in NMR.

Among various ways to increase NMR sensitivity, one particular approach based on the combination of NMR with the use of parahydrogen (p-H_2) is rather unique and is particularly suitable for studying reactions that involve molecular hydrogen. An important prerequisite is that the two H atoms of a p-H_2 molecule do not lose each other in a catalytic cycle and end up in the same product molecule or a reaction intermediate. In such a case, the correlated spin state of the two H atoms in a p-H_2 molecule can convert into parahydrogen-induced polarization (PHIP) of nuclear spins in the reaction products or intermediates if the reaction causes the two H atoms to become inequivalent. Fig. 1 shows schematically how such experiments are implemented in practice [1].

The parahydrogen-based enhancement of NMR signals of the reaction products and intermediates has been first demonstrated in homogeneous hydrogenations of unsaturated compounds by transition metal complexes in solution [2]. This opened the way to the sensitive NMR studies of the mechanisms of H_2 activation by transition metal complexes with the formation of dihydride or polyhydride species, their transformations, and interactions with unsaturated substrates to produce hydrogenation products [3]. A recent example of such study [4] is presented in Fig. 2.

Understanding heterogeneous catalytic processes at the same level of detail is significantly more challenging, in particular because such systems usually possess several different types of active centers acting in parallel, the surface structure can evolve under the reaction conditions, the catalyst support may be involved in the reaction, etc. At the same time, heterogeneous catalytic processes largely prevail in industrial catalysis, and it is thus highly desirable to develop advanced in situ and operando methods for their characterization.

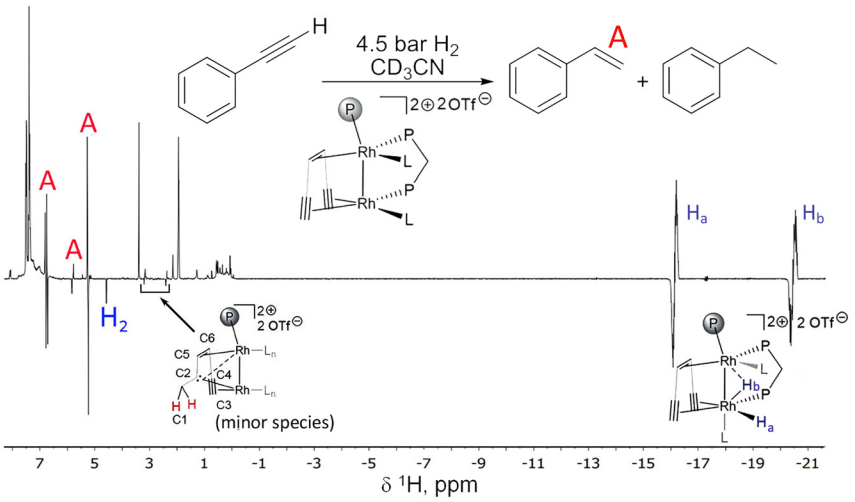

Fig. 2: The reaction scheme for hydrogenation of phenylacetylene with parahydrogen over homobimetallic Rh complex in CD_3CN, and the corresponding ^{1}H NMR spectrum acquired in a PASADENA experiment. The NMR signals of the product styrene (labeled A), the dihydride intermediate (H_a, H_b), a minor Rh species (due to minor amounts of diphosphine-ligand-free complex present in the sample), and orthohydrogen (H_2) demonstrate enhanced NMR signals in the spectrum. L = CD_3CN; the other two ligands, namely 10,11-di-(trimethylsilyl)acetylene-5H-dibenzo[a,d]cyclohepten-5-diphenylphosphine and bis(diphenylphosphino)methane, are presented in a simplified form in the structures shown in the figure. Adapted from [4] with permission from The Royal Society of Chemistry.

HET-PHIP: from immobilized metal complexes to surface organometallic chemistry

Parahydrogen-based NMR signal enhancement effects with the use of heterogeneous catalysts were not observed until 2007, nor were they expected in heterogeneous catalytic processes. In the end, it was a matter of building yet another bridge between homogeneous and heterogeneous catalysis. Even if naïve, the initial idea was to utilize the ability of transition metal complexes to produce parahydrogen-induced polarization effects in solution and to turn these homogeneous catalysts into their heterogeneous counterparts by immobilizing them on suitable porous supports. After numerous unsuccessful attempts, this approach was finally demonstrated successfully with Wilkinson's catalyst immobilized on either styrene-divinylbenzene polymer or on silica gel in the hydrogenation of styrene to ethylbenzene [5, 6]. However, immobilized metal complexes are known to leach from the solid support into solution when they are used in catalytic processes in the liquid phase [7]. Therefore, while the required tests for potential leaching were successfully performed, the very first demonstration of heterogeneous PHIP (HET-PHIP), to be absolutely reliable, required a more unambiguous confirmation. This was achieved by excluding any liquid phase in the experiments with gaseous substrates, namely hydrogenation of propylene to propane [5, 6]. The successful observation of PHIP in those experiments has proven beyond doubt that HET-PHIP effects are indeed feasible with the properly designed catalysts. Furthermore, some useful mechanistic information can be obtained from their observation. For instance, while hydrogenation of propyne leads to the same product (propylene) for both syn- and anti-addition of H_2 to the substrate, the two reaction routes yield different PHIP patterns in the ^{1}H NMR spectra, which allowed to conclude that immobilized Rh complexes operate via syn-addition of H_2 [8]. The use of other immobilized Wilkinson's type catalysts in similar studies has been reported by others as well [9, 10]. PHIP effects were also observed with several cationic Rh complexes immobilized on silica gel [5, 6, 8]. However, in most, if not all, cases, the performance of the catalysts was relatively poor because of metal leaching in liquid–solid processes and chemical degradation in gas–solid reactions at elevated temperatures in the presence of H_2.

Similar problems were encountered in the PHIP studies that used immobilized Ir complexes [11]. At the same time, some of the Ir-based catalysts were markedly more stable compared to Rh-based systems. In particular, $[Ir(CO)(PPh_3)_2Cl]$ (Vaska's complex) immobilized on phosphine-modified silica was able to produce PHIP effects while demonstrating reasonable stability up to 140 °C in H_2-rich gas mixtures [12]. An example of the studies involving an immobilized [Ir(COD)(phosphine)Cl] catalyst is shown in Fig. 3.

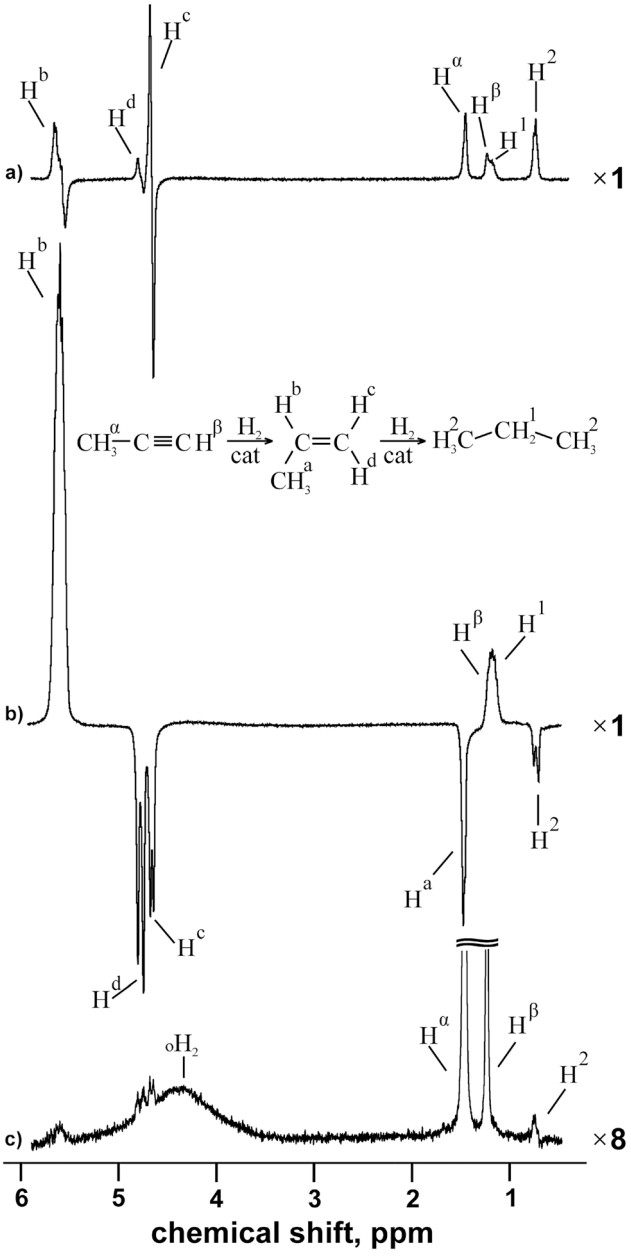

Fig. 3: ^{1}H NMR spectra of the reaction mixture acquired during the gas-phase heterogeneous hydrogenation of propyne over the immobilized Ir complex prepared from chloro(1,5-cyclooctadiene)iridium(I) dimer, dehydrated silica gel and the bifunctional linker ligand 2-(diphenylphosphino)ethyltriethoxysilane. The a) PASADENA and b) ALTADENA experiments were conducted at 80 °C. Spectrum c) was acquired several seconds after interrupting gas flow in the ALTADENA experiment; the broad peak labeled oH_2 corresponds to orthohydrogen, and the signals H^{α} and H^{β} of propyne are clipped for a better visibility of the signals of the reaction products. The scaling factors for the spectra are shown to the right of the individual spectra. Reprinted from [11] copyright 2013 with permission from Springer Nature.

The same approach was extended to other types of immobilized metal complexes. In particular, to establish the role of cationic gold in catalytic processes, a catalyst comprising a complex of Au(III) with a Schiff base immobilized on an organometallic substrate (IRMOF-3-Si-Au) was tested. Hydrogenation of propylene and propyne on this catalyst was carried out using parahydrogen, which demonstrated that IRMOF-3-Si-Au hydrogenates propylene to propane, and pronounced PHIP effects are observed when one uses parahydrogen in this reaction [13].

A different immobilization strategy that uses supported ionic liquid phase (SILP) was employed to support a cationic Rh complex on silica gel [14]. This catalyst produced PHIP effects in hydrogenation of propylene with p-H_2, but the NMR signal enhancement dropped from 200–400 to 10–20 after about 10 min. A pronounced activation period was observed for this catalyst, which likely indicates chemical transformation of the initial immobilized complex during catalyst activation.

Immobilization of metal complexes on solid supports is certainly not a new approach in modern catalysis. A lot of work done in this field has revealed many problems with such materials. In addition to leaching mentioned above, such catalysts can be rather unstable and deactivate easily under reactive conditions, especially in the gas-phase processes performed at elevated temperatures. In fact, at least in some of the systems described above, it is possible that PHIP effects were observed owing to the reduction of the original metal complexes and formation of metal nanoparticles (NP) (see below). This possibility has not been considered in any detail at that time because PHIP effects on supported metals were then unknown and were considered impossible.

In an attempt to design better catalysts, a more recent trend in modern catalysis uses surface organometallic chemistry (SOMC) to design well-defined active centers on solid materials that would have a specific and reasonably stable structure and provide efficient performance in the catalytic processes. In line with this trend, single-site catalysts constructed by means of SOMC were tested in hydrogenations of unsaturated compounds with parahydrogen. For instance, a silica-supported vanadium oxo organometallic complex was tested in the hydrogenation of propyne and propylene with parahydrogen [1]. This group 5 metal catalyst demonstrated NMR signal enhancements of 200–300-fold in the case of propylene hydrogenation to propane and ca. 1300-fold in the case of propyne hydrogenation to propylene (Fig. 4).

HET-PHIP: from supported metal nanoparticles to single-atom catalysts

The observation of PHIP effects usually requires pairwise addition of H_2 to a substrate. i. e., both H atoms of a single H_2 molecule should stay close to each other throughout the catalytic cycle all the way from the moment of H_2 activation to the incorporation of its two H atoms in the product molecule. Such a reaction mechanism is usually associated with homogeneous hydrogenation through the formation of a dihydride metal complex, and indeed, as mentioned above, PHIP effects were originally observed in homogeneous hydrogenations catalyzed by transition metal complexes, and later successfully extended to immobilized metal complexes. At the same time, metals (e. g., supported metal nanoparticles) are expected to operate via an entirely different mechanism, by dissociatively chemisorbing H_2 and then incorporating random H atoms into the substrate molecule to yield the hydrogenation product. The migration of H atoms on metal surfaces is extremely rapid, with jumps between the neighboring metal atoms being on the sub-nanosecond timescale for Pt group metals [15]. This fact was expected to prevent entirely the pairwise addition of H_2 on metal surfaces, which is the

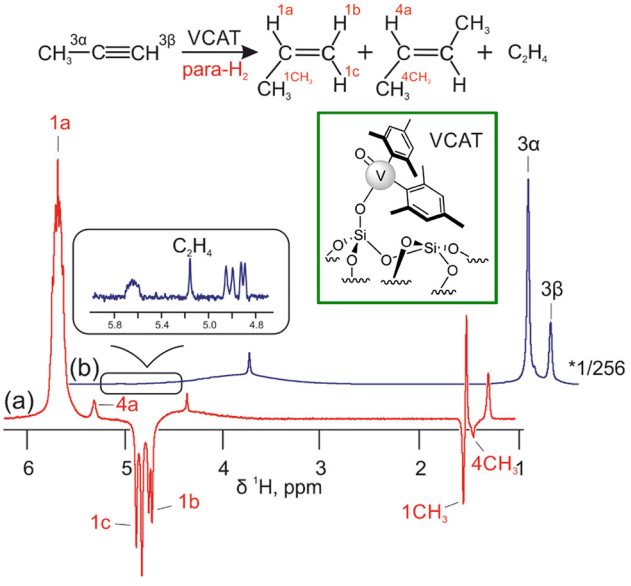

Fig. 4: The reaction scheme for propyne hydrogenation with p-H_2 over silica-supported vanadium oxo organometallic complex (VCAT), and the corresponding ^{1}H NMR spectra detected in the ALTADENA experiment. The reaction was performed at 500 °C by supplying a 1:4 propyne:p-H_2 mixture to the reactor at the flow rate of 2.1 scc/s. Spectrum (a) was detected in the continuous flow mode using a single scan, whereas for (b) 256 scans were accumulated after gas flow was abruptly terminated. The structure of the catalyst is schematically shown in the inset. Adapted with permission from [1]. Copyright 2018 American Chemical Society.

reason why PHIP effects were not considered feasible in heterogeneous hydrogenations. Therefore, it came as a big surprise when HET-PHIP effects were for the first time demonstrated with the use of supported metal catalysts such as Pt/Al_2O_3 and Pd/Al_2O_3 [16]. These observations established the fact that centers of pairwise H_2 addition do exist on supported metal catalysts, which was a rather unexpected result. Furthermore, already in the first published study the dependence of NMR signal enhancement on the Pt nanoparticle size was revealed, making it clear that HET-PHIP over supported metals is a very complex phenomenon.

Subsequent studies addressed in detail the dependence of the efficiency of pairwise addition of a parahydrogen molecule to a substrate molecule on the type of metal [17–19] and its redox state [18], metal nanoparticle size [17, 20] and shape [21], metal loading [19], the nature of support [17, 22] and the effect of strong metal-support interaction [23]. HET-PHIP effects also have a pronounced dependence on the nature of the substrate used in the hydrogenation with parahydrogen. As an example of a substrate possessing conjugated multiple bonds, hydrogenation of 1,3-butadiene was studied on supported Pt catalysts [24]. The reaction led to the formation of multiple reaction products (1-butene, 2-butene, butane), and all these products exhibited PHIP effects. These results imply that, in addition to hydrogenation of 1,3-butadiene to 1-butene, isomerization and subsequent hydrogenation (possibly also pairwise) lead to the formation of 2-butene and butane, respectively. The largest PHIP effects were observed with the Pt catalyst supported on TiO_2, similar to the hydrogenation of propylene. In contrast, for supported palladium catalysts (Pd/Al_2O_3, Pd/SiO_2, Pd/ZrO_2) with different metal particle sizes, of all reaction products only the product of partial hydrogenation (1-butene) was showing PHIP effects. However, with Pd/TiO_2 catalyst all the reaction products (1-butene, 2-butene, butane) were polarized in the hydrogenation reaction of 1,3-butadiene with parahydrogen (Fig. 5). This once again confirms the fundamental influence of the nature of the support on the catalytic properties of the supported metal. Pt and Pd catalysts supported on Al–Si and Zr-Si fibers were also studied using the HET-PHIP approach [25], demonstrating that pairwise addition of H_2 on such catalysts is also feasible.

Rhodium catalysts were also addressed in the context of HET-PHIP studies, and it was found that Rh/TiO_2 was the most efficient in terms of PHIP, and 1 wt.% Rh/TiO_2 catalyst with 0.7 nm Rh nanoparticles demonstrated efficiency similar to that of the most efficient Pt catalyst (Pt/TiO_2, 0.7 nm Pt particle size). This catalyst was used in particular in the heterogeneous liquid-phase hydrogenation of propylene, acrylamide and styrene [26], demonstrating their successful catalytic conversion to the respective products. Moreover, when

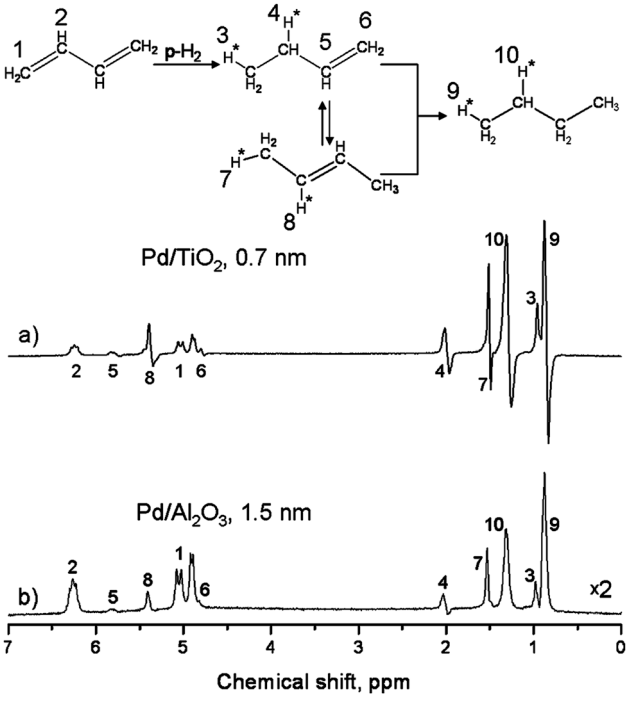

Fig. 5: The reaction scheme for the hydrogenation of 1,3-butadiene with p-H_2, and the ^{1}H NMR spectra detected in the PASADENA experiment while the reaction was performed at 100 °C over (a) Pd/TiO_2 catalyst and (b) Pd/γ-Al_2O_3 catalyst. The selective pairwise hydrogen addition to 1,3-butadiene over supported Pd/TiO_2 catalyst leads to the formation of polarized butane, 1-butene and 2-butene, whereas over Pd/γ-Al_2O_3 only 1-butene is polarized. The ^{1}H NMR signals of all compounds are labeled as indicated in the figure. Reprinted with kind permission from Springer-Verlag: Ref. [24], Figure 14.

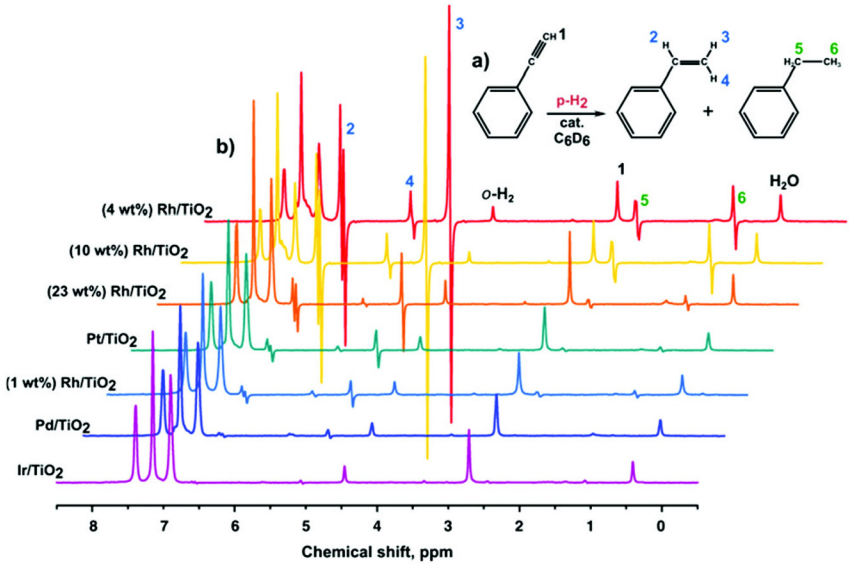

Fig. 6: a) The reaction scheme of phenylacetylene hydrogenation with parahydrogen. b) ^{1}H NMR spectra acquired during the reaction carried out over several different heterogeneous catalysts (specified in the figure) in a PASADENA experiment. The spectra are arranged (top to bottom) from the highest to the lowest value of the observed PHIP effect. Reproduced from Ref. [19] with permission from the PCCP Owner Societies.

parahydrogen was used in the reaction, it was possible to observe polarized NMR lines of the products. A recent study compared several metal catalysts supported on titania in the liquid phase hydrogenation of phenylacetylene (Fig. 6) and other phenylalkynes in more detail [19]. The results on liquid-phase hydrogenation with parahydrogen on supported metal catalysts open wide prospects for the use of the resulting polarized liquids in various MRI applications.

Gas-phase hydrogenation of furan, 2,3-dihydrofuran (2,3-DHF) and 2,5-dihydrofuran (2,5-DHF) was addressed using 1, 10, and 20 wt.% Rh/TiO_2 catalysts, 1 and 10 wt.% Pt/TiO_2 and 1% wt.% Pd/TiO_2 catalysts [27]. For all three Rh/TiO_2 catalysts, intense hyperpolarized signals of tetrahydrofuran (THF) were observed in ^{1}H NMR spectra acquired during furan hydrogenation. In addition, weaker polarized lines of the CH_2 groups of the partial hydrogenation product 2,3-DHF were detected. In contrast, hydrogenation of furan on a 1 wt.% Pd/TiO_2 catalyst produced no PHIP effects despite the formation of THF as a reaction product. When 2,3-dihydrofuran was hydrogenated with parahydrogen on Rh/TiO_2 catalysts, polarized signals were observed for THF (Fig. 7). However, the most interesting fact is that ^{1}H NMR signal polarization was also detected for CH groups of the

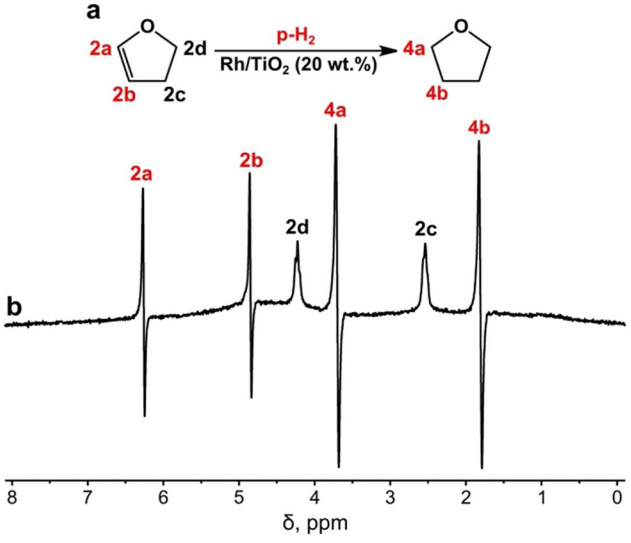

Fig. 7: a) The reaction scheme for the hydrogenation of 2,3-dihydrofuran with p-H_2, and b) the ^{1}H NMR spectrum acquired for the reaction performed at 130 °C and a 2.5 ml/s gas flow rate over 20 wt.% Rh/TiO_2 catalyst. Reproduced from ref. [27] with permission of WILEY-VCH Verlag GmbH & Co. KGaA, Weinheim.

reagent (2,3-DHF), while the signals of the CH_2 groups of this compound remained unenhanced. This can be explained by the pairwise exchange or replacement phenomenon, which was previously demonstrated for the hydrogenation of propylene on supported metal catalysts and on ceria. This mechanism involves several steps of adding and removing the H atoms through the formation of surface species of trihydrofuran. In the hydrogenation of 2,5-DHF over Rh/TiO_2 catalysts, PHIP effects were observed both for THF and 2,3-DHF. Moreover, in the case of the 1 wt.% Rh/TiO_2 catalyst, all the NMR signals of 2,3-DHF were polarized, in contrast to the results obtained for hydrogenation of 2,3-DHF. The formation of 2,3-DHF is apparently associated with the isomerization of 2,5-DHF. It is important to note that 2,3-DHF molecules in the case of rhodium catalysts demonstrated the PHIP effects for all protons, which is most likely due to the dehydrogenation of 2,5-DHF to furan and the subsequent pairwise addition of parahydrogen.

Reactions of unsaturated cyclic compounds were exemplified by the gas-phase hydrogenation of benzene and several other six-membered cyclic compounds, such as toluene, cyclohexene, and 1,3- and 1,4-cyclohexadiene over Rh/TiO_2, Pt/TiO_2, and Pt/TiO_2 catalysts [28]. Regardless of the nature of the catalyst used, the same sets of hydrogenation products were observed. Neither benzene nor toluene yielded any polarization for the reaction products, implying that their hydrogenation does not involve pairwise H_2 addition. One possibility is that the reaction proceeds via 1,4-hydrogenation as the first step, which cannot occur in a pairwise manner on a metal surface. In contrast, hydrogenation of cyclohexene and cyclohexadienes did produce PHIP effects for the reaction products. Another cyclic compound that was hydrogenated with parahydrogen is cyclopropane. This reaction produced an unexpected polarization pattern for the reaction product propane [29]. In this case, addition of two H atoms of the H_2 molecule to the same carbon atom of the reactant (cyclopropane) should not produce any observable PHIP effects even if the addition of H_2 is pairwise because the two H atoms remain equivalent in the product molecule. Therefore, the observation of PHIP effects for propane in this reaction implies a certain sequence of molecular transformations, providing a useful mechanistic insight. In addition, this process may serve as an alternative route toward highly polarized propane gas for its applications in combination with MRI detection.

One of the trends in catalysis is the reduced utilization of noble metals. For instance, copper-based catalysts are a cheaper and useful alternative. Along these lines, it was found that surface modification of Cu/SiO_2 catalysts with phosphine ligands makes it possible to produce chemo- and stereoselective catalysts for hydrogenation of alkynes [30]. It was found that the Cu/SiO_2 catalyst is quite active in the gas-phase hydrogenation of 1-butyne at 350–550 °C, accompanied by a fairly high conversion (37–81%). It is important that the catalyst has a high selectivity for the formation of 1-butene (about 97%). Moreover, the PHIP effects were observed for all protons of the resulting 1-butene when parahydrogen was used in the reaction (Fig. 8). The Cu/SiO_2 catalyst was also investigated in the hydrogenation of 2-butyne. While the formation of 2-butene and butane proceeded efficiently at 250–350 °C, no PHIP effects could be observed, which may indicate that two or more different catalytically active centers are available on these catalysts.

A different study [31] addressed a series of catalysts comprising Co and Ni nanoparticles supported on SiO_2, Al_2O_3 and TiO_2 in the hydrogenation of propylene at 500 °C. Cobalt supported on SiO_2 showed low activity and very small PHIP effects, but the same metal supported on Al_2O_3 was measurably more active and demonstrated clear PHIP effects. Furthermore, similar to other supported metals, cobalt on titania demonstrated much more substantial PHIP effects, and also was active even at a lower temperature of 400 °C. The apparent pairwise H_2 addition selectivity for Co/TiO_2 was estimated as 2–3%, but the actual value was likely significantly higher. Indeed, when inevitable polarization losses were taken into account by introducing appropriate corrections, the values increased to 19–25%. Such a high level of pairwise selectivity may be associated with the Co nanoparticles smaller than 0.5 nm. In contrast, while supported Ni catalysts demonstrated substantially higher conversions in the hydrogenation of propylene, they also catalyzed side reactions, e. g., hydrocarbon cracking into methane and ethane. PHIP effects were observed with Ni/Al_2O_3 and Ni/TiO_2 catalysts but not with Ni/SiO_2, but the pairwise selectivity was much lower compared to the Co catalysts. In any case, observation of PHIP effects over Co and Ni nanoparticles is an important finding. Indeed, magnetic materials cause accelerated relaxation of nuclear spins in the molecules they are in contact with; for instance, paramagnetic gadolinium chelates and superparamagnetic nanoparticles used in contrast-enhanced medical MRI is one such example of

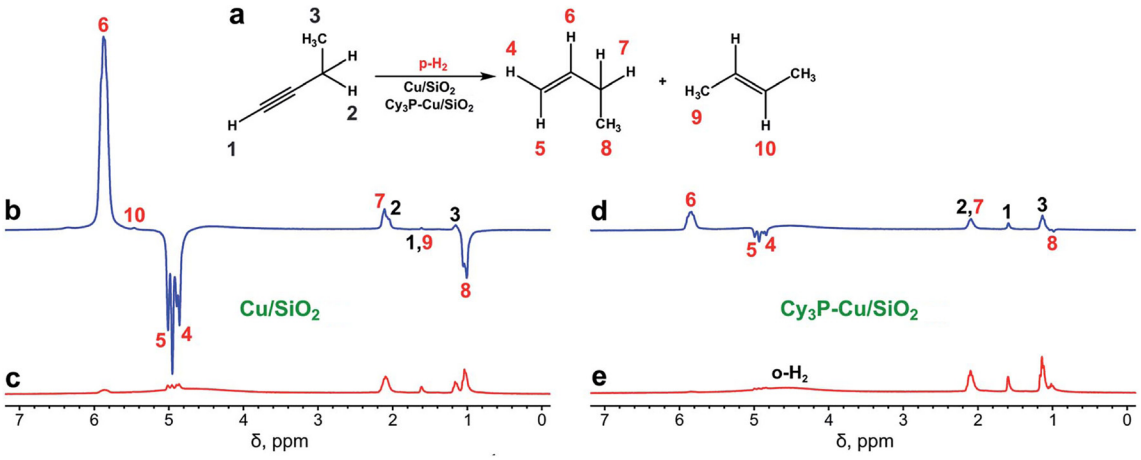

Fig. 8: a) The reaction scheme of 1-butyne hydrogenation with p-H_2, and b–e) the ^{1}H NMR spectra acquired during the reaction (b,d) while the gas was flowing and (c, e) after rapid interruption of the gas flow and subsequent relaxation of nuclear spins to thermal equilibrium. The reaction was carried out using (b, c) the unmodified Cu/SiO_2 catalyst or (d, e) catalyst modified with the tricyclohexylphosphine ligand ($Cy_3P–Cu/SiO_2$). In these ALTADENA experiments, the reaction temperature was 450 °C, and gas flow rate was 5.1 ml/s. All spectra were acquired with 8 signal accumulations and are presented on the same vertical scale. Reproduced from [30] with permission from The Royal Society of Chemistry.

practical importance. As a result, the magnetic nature of a catalyst was deemed to be an obstruction that could make PHIP effects unobservable because of the very rapid polarization loss induced by such catalysts. The small Co and Ni nanoparticles are likely superparamagnetic under the experimental conditions used, showing that the magnetic nature of a catalyst does not necessarily preclude the formation and observation of PHIP effects. Furthermore, as discussed in the next section, PHIP effects were also successfully observed with the use of paramagnetic Cr_2O_3 as hydrogenation catalyst. All these observations potentially extend the applicability of the PHIP technique to the studies of processes that involve magnetic materials. At the same time, while magnetic ortho-para conversion of H_2 is well known and thoroughly studied [32, 33], local magnetic fields may affect nuclear spin states of hydrogens produced upon catalytic activation of H_2 very differently from those in the intact H_2 molecule. Thus, currently any extensive discussion of PHIP effects produced with magnetic catalysts is not possible until the results of dedicated studies addressing both the PHIP effects and the magnetic properties of the catalysts become available in the future.

Despite a substantial amount of research performed in the field of HET-PHIP, there remain a large number of questions yet to be answered. This includes the key puzzle of what makes HET-PHIP possible upon hydrogenation on metal surfaces. An early (and perhaps rather naïve) explanation involved partitioning of the metal surface into smaller areas by the adsorbed species such as reactants, intermediates, spectators, carbonaceous deposits, etc. This partitioning was expected to reduce the mobility of hydrogen atoms on the metal surface to the extent that it would force the two H atoms formed upon H_2 dissociation to stay together until they end up in the product molecule. However, till this day it was not possible to reliably confirm or disprove this hypothesis. In some studies, ligands such as thiols adsorbed on metal NPs seem to measurably increase the pairwise selectivity of metal catalysts [34, 35]. However, this in itself does not prove that the improved behavior is the result of reduced surface mobility of hydrogen atoms. More likely, the catalytic poisons suppress the activity of less selective catalytic sites to a larger extent compared to that of more selective catalytic centers, as it is the case in many other examples in heterogeneous catalysis when catalysts are heavily poisoned to improve selectivity at the expense of a major reduction in conversion.

In any case, supported and unsupported metal catalysts cannot achieve ultimate signal enhancement combined with a high catalytic conversion. The likely reason is that pairwise H_2 addition route on such catalysts is not the main reaction mechanism, and that most of the reaction product is produced via addition of random H atoms to a substrate, in line with the original expectations. While varying the metal catalyst

composition and structure, catalyst synthesis and pre-treatment procedures, the nature of catalyst support, the type of substrate, reaction conditions, etc., can improve somewhat the pairwise selectivity of the catalyst and thus increase the observed effects, achieving the ultimate performance in terms of conversion and pairwise selectivity may require an entirely different approach.

Higher atomic efficiency of the utilization of expensive metals is deemed achievable by exposing more metal atoms via the reduction of metal nanoparticle size, down to the size of a monoatomic metal distribution on a support in single atom catalysts (SAC). In addition, this ultimate size reduction invokes quantum effects and more intimate metal-support interactions that may significantly alter catalyst performance. The key problem encountered on this way is the inherently unstable character of single metal atoms which exhibit tendency to aggregate into clusters. The support thus serves a major purpose of stabilizing single metal atoms on its surface to mitigate this tendency to aggregation. Furthermore, the support atoms that surround the metal center contribute to the structuring of a catalytically active site and in some cases play an active role in the catalytic process. To this end, suitable inorganic or organic supports are utilized that include, for instance, appropriate metal oxides, sulfides, carbides and nitrides, a variety of carbon-based materials, MOFs, various polymeric matrices, etc. A somewhat different approach uses dilution of a catalytically active metal in a second metal with a much lower activity in metal alloys, known as single-atom alloy (SAA) catalysts.

Similar to catalytic applications, the concept of SAC is very attractive for parahydrogen-based NMR signal enhancement. Indeed, as discussed above, the major drawback of supported metal NPs for such applications is the very rapid migration of hydrogen atoms on their surfaces which leads to low pairwise selectivity in H_2 addition. It can be expected that as the size of a metal NP is reduced, the diffusive separation of H atoms on the catalyst should be significantly inhibited by a variety of factors, from simple geometric restrictions to quantum and electronic effects that change the adsorption energy and diffusion barriers as the metal NP shrinks. In the ultimate limit of a single metal atom, the catalyst behavior may be expected to mimic that of metal complexes in homogeneous hydrogenations in solution, i. e., to favor pairwise H_2 addition to a substrate.

It is thus not surprising that a number of studies report the use of SAC and related catalysts in the hydrogenations with parahydrogen. The first study that used SACs in the context of parahydrogen [36] addressed hydrogenation of 1,3-butadiene and 1-butyne over the catalyst comprising single gold atoms dispersed on multiwalled carbon nanotubes. The study demonstrated the anticipated higher contribution of pairwise H_2 addition on these single-atom catalytic centers (in excess of 10%) compared to supported metal catalysts. Single gold atoms dispersed on N-doped carbon is another system that was addressed in the context of selective semihydrogenation of alkynes to alkenes [37], and demonstrated some NMR signal enhancement in the experiments with parahydrogen. At the same time, the activity of the single atom Au catalysts was relatively low, providing very little hydrogenation product under the experimental conditions used, which makes them not particularly suitable for many parahydrogen-based applications. Indeed, in addition to a high degree of pairwise H_2 addition, a catalyst needs to demonstrate a substantial (tens of %) substrate-to-product conversion within a relatively short (seconds) contact time between the reactants and the catalyst. Thus, catalysts based on metals such as Au and Ag, even if active in the hydrogenation reactions when finely dispersed, may not be suitable for achieving the best performance in the processes involving parahydrogen.

One of the other representative examples is the catalyst possessing well-defined isolated Co(II) sites on the surface of silica support [38]. Heterogeneous hydrogenation of propylene was carried out using this catalyst, demonstrating that it is active in this reaction. Observation of polarized antiphase propane signals when parahydrogen was used in the reaction is a direct evidence that pairwise pathway of molecular hydrogen addition is taking place to some extent. Similar studies were performed with a catalyst possessing isolated Cr(III) centers on the surface of silica, alumina, or silica-alumina supports [39]. The results showed that, similar to the isolated Co(II) centers, Cr(III) centers on the surface of a porous support can partially implement pairwise H_2 addition to unsaturated substrates.

As platinum group metals are inherently more active in catalytic transformations, it appeared reasonable to test them in HET-PHIP experiments. In particular, a single-atom palladium catalyst prepared by anchoring of Pd atoms into the cavities of mesoporous polymeric graphitic carbon nitride [40, 41] was also tested in the

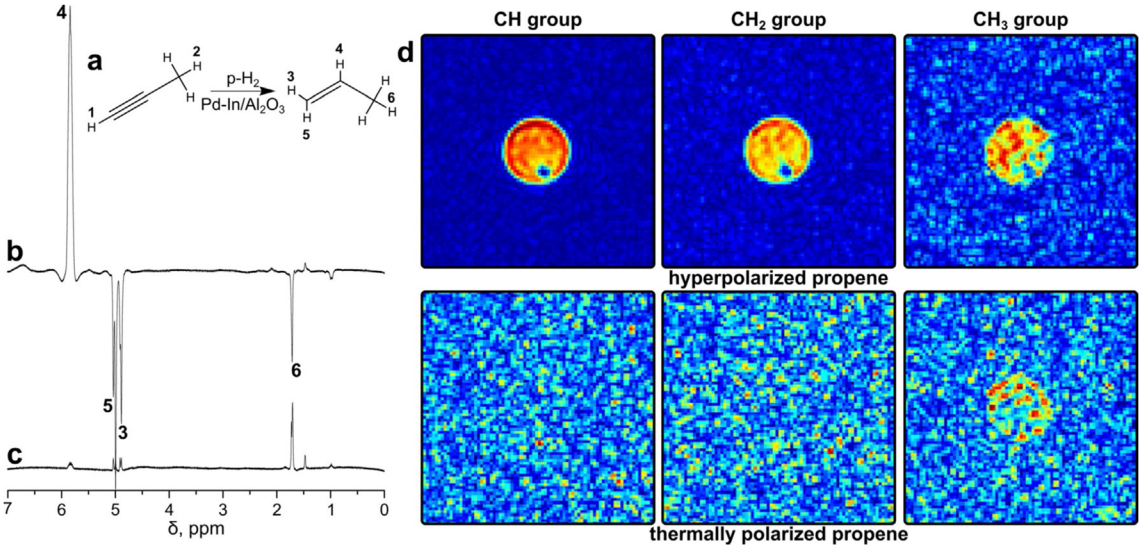

Fig. 9: (a) The reaction scheme for propyne hydrogenation with p-H_2 over Pd-In/Al_2O_3 catalyst. (b), (c) ^{1}H NMR spectra acquired during the reaction (b) while the gas was flowing and (c) after an abrupt interruption of the gas flow and the subsequent relaxation of nuclear spins to thermal equilibrium. In this ALTADENA experiment, the reaction temperature was 400 °C, and the gas flow rate was 8.8 ml/s. (d) Transverse MR images of a 10 mm NMR tube filled with propylene in thermal equilibrium (bottom row) or hyperpolarized (top row) propylene. MR images of hyperpolarized propylene were acquired while the gas was flowing, separately for each of the three groups of hydrogen atoms in the propylene molecule. For all MR images, the matrix size and spatial resolution were equal to 64 × 64 and 0.8 × 0.8 mm^2 per pixel, respectively. Reproduced from ref. [43] with permission of WILEY-VCH Verlag GmbH & Co. KGaA, Weinheim.

liquid- and gas-phase hydrogenation of alkynes with parahydrogen and demonstrated some NMR signal enhancements, albeit not as high as one might expect for such catalysts. Another interesting system is based on the single Pd atoms dispersed on a nanodiamond/graphene hybrid support, which demonstrates high activity and selectivity in hydrogenation of acetylene to ethylene [42], and is also demonstrating pronounced PHIP effects.

The promising potential of the SAA-type catalysts in the context of HET-PHIP research and practice was recently demonstrated with the use of a Pd-In/Al_2O_3 catalyst [43]. As a result of isolation of Pd sites by In atoms, the Pd-In/Al_2O_3 catalyst demonstrated high activity and selectivity to propylene in the gas-phase semi-hydrogenation of propyne. The formation of Pd-In intermetallic compound during catalyst reduction was verified by XPS. This catalyst produced rather strong PHIP effects upon propyne hydrogenation with para-hydrogen (Fig. 9), and the selectivity to pairwise H_2 addition estimated by taking into account the relaxation losses amounted to ca. 9.3%. The very high value of NMR signal enhancement in combination with significant catalytic conversion (ca. 20%) allowed the authors to produce significant amounts of highly hyperpolarized gas and to perform MRI of flowing hyperpolarized propylene with 0.8 × 0.8 mm^2 spatial resolution, selectively for each of the three groups of hydrogen atoms of propylene. This would be impossible to achieve with thermally polarized propylene under the same conditions.

HET-PHIP: metals vs. metal oxides, sulfides and carbides

It is known that various metal oxides are capable of catalyzing hydrogenation of unsaturated hydrocarbons. The possibility of using metal oxide catalysts to produce hyperpolarized substances during hydrogenation with parahydrogen was thus investigated [44]. Propylene and 1,3-butadiene were hydrogenated with para-hydrogen on oxides such as CaO, Cr_2O_3, and CeO_2. It was shown that hydrogenation of 1,3-butadiene produced

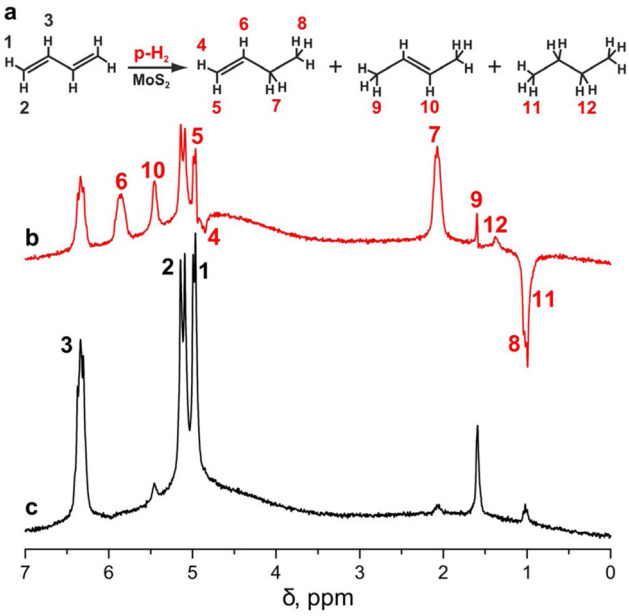

Fig. 10: a) The reaction scheme of 1,3-butadiene hydrogenation with p-H_2 over MoS_2/γ-Al_2O_3 catalyst. b, c) ^{1}H NMR spectra acquired in the ALTADENA experiment during the reaction performed at 500 °C (a) while the gas was flowing at 4 ml/s and (b) after gas flow termination. The spectra were acquired with 16 signal accumulations each and are presented on the same vertical scale. Reproduced from ref. [47] with permission of WILEY-VCH Verlag GmbH & Co. KGaA, Weinheim.

fairly intense polarized signals of 1-butene, 2-butene and butane in the ^{1}H NMR spectra. PHIP effects were also observed in the hydrogenation of 1,3-butadiene and 1-butyne over bulk PtO_2 and $Pt(OH)_2$ catalysts, as well as over platinum black. At the same time, among similar palladium catalysts (PdO, $Pd(OH)_2$, Pd black), polarized signals in the NMR spectra could be observed only for PdO, but not for Pd and $Pd(OH)_2$. Such a prominent difference in the behavior of platinum and palladium can be due to the fact that bulk palladium easily forms hydride phase, which leads to a loss of spin correlation between hydrogen atoms and makes it impossible to observe PHIP effects.

PHIP effects over CeO_2 catalysts were later studied in more detail. To this end, ceria nanoparticles with different crystalline facets (cubes, octahedral and rods) were synthesized and studied in the hydrogenation of propyne and propylene with parahydrogen [45, 46]. The pairwise selectivity of propyne hydrogenation was reported to be strongly shape dependent, with hydrogenation over oxygen-deficient facets of CeO_2 rods providing the highest pairwise H_2 addition selectivity, and yielding important information on the reaction mechanism for hydrogenations catalyzed by ceria. Interestingly, in the case of propylene hydrogenation, PHIP effects were observed not only for propane, but also for propylene itself, interpreted as the result of pairwise hydrogen replacement process in the substrate molecule.

PHIP effects were also successfully observed for hydrogenations over molybdenum sulfide catalysts, which made it possible to employ the PHIP technique to address hydrodesulfurization processes [47]. It is often assumed that hydrodesulfurization of the model compound thiophene can proceed along two possible routes, namely the hydrogenation route and the direct hydrodesulfurization route. A typical catalyst for the hydrodesulfurization of thiophene is molybdenum disulfide supported on γ-Al_2O_3. The main products of thiophene hydrodesulfurization reaction on the MoS_2/γ-Al_2O_3 catalyst were 1-butene, 2-butene and butane. However, all attempts to detect any PHIP effects were not successful under various conditions. As noted above, hydrodesulfurization of thiophene can proceed along two different routes: 1) via hydrogenation of thiophene to dihydrothiophenes and tetrahydrothiophene with subsequent elimination of sulfur; and 2) via direct hydrodesulfurization of thiophene with the formation of 1,3-butadiene and hydrogen sulfide, followed by hydrogenation of 1,3-butadiene to butenes and butane. In order to establish which route is implemented in this catalytic system, 1,3-butadiene was hydrogenated with parahydrogen over a MoS_2/γ-Al_2O_3 catalyst (Fig. 10). In the ^{1}H NMR spectra of the reaction mixture, characteristic PHIP signals were observed for various reaction products (1-butene, 2-butene and butane). Thus, the PHIP effects would be observable if the thiophene hydrodesulfurization reaction proceeded via the direct desulfurization route, i. e., via formation of

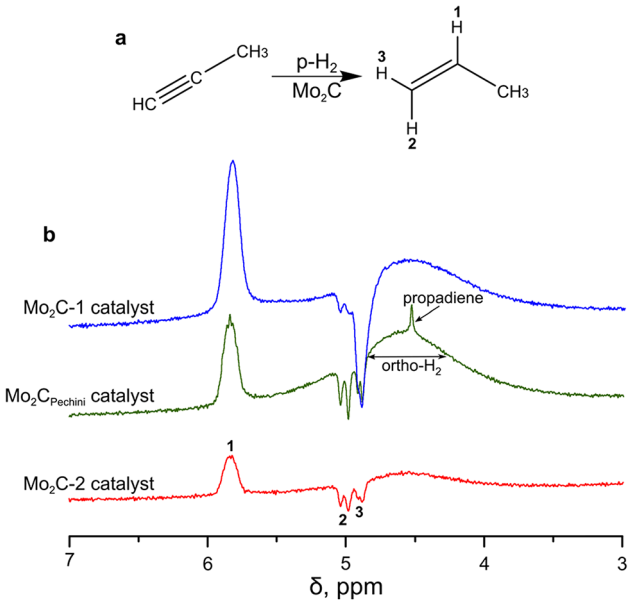

Fig. 11: a) The reaction scheme of propyne hydrogenation with p-H_2 over the Mo_2C catalysts. b) The ^1H NMR spectra acquired in the ALTADENA experiment during the reaction while the gas mixture was flowing at 5.1 ml/s. The catalysts were prepared either using temperature-programmed reduction of commercial MoO_3 (catalysts Mo_2C-1 and Mo_2C-2) or the Pechini synthesis from $(NH_4)_6Mo_7O_{24} \times 4H_2O$ ($Mo_2C_{Pechini}$). Note that for Mo_2C-1 the syn addition of H_2 dominates (signals 1 and 3 are predominantly enhanced), whereas other two catalysts are able to efficiently perform cis-trans isomerization of the C=C bond of propylene product. Catalyst $Mo_2C_{Pechini}$ is active in isomerizing propyne into propadiene. Reprinted from [48] copyright 2018 with permission from Springer Nature.

1,3-butadiene and its subsequent hydrogenation. Since no PHIP effects were observed during hydrodesulfurization of thiophene on MoS_2/γ-Al_2O_3, it can be assumed that 1,3-butadiene is not formed in this catalytic process, that is, the main pathway for hydrodesulfurization of thiophene on the MoS_2/γ-Al_2O_3 catalyst is the hydrogenation of thiophene.

Metal carbides can be active hydrogenation catalysts, and were also tested in the context of HET-PHIP studies. It was demonstrated in particular that the phase composition of molybdenum carbide catalysts has a pronounced influence on the PHIP effects observed upon gas-phase hydrogenation of propyne with parahydrogen [48]. Specifically, the catalysts were produced using different synthetic procedures, and predominantly contained either a fcc MoC_{1-x} phase or a hcp Mo_2C phase. It was found in this study that the catalysts with the dominating hcp Mo_2C phase provided a higher contribution of pairwise H_2 addition to propyne, yielding a ca. 150-fold proton NMR signal enhancement (Fig. 11).

HET-PHIP: potential applications

MR imaging of catalytic reactors [49–52] using gases is much more demanding compared to imaging of liquids because the spin density in the gas phase is 3 orders of magnitude lower than in the condensed phase. This severely limits the use of MRI for studies involving gases. NMR signal enhancement provided by the PHIP effect can significantly advance gas-phase MRI studies. The first MRI experiments that utilized hyperpolarized fluids produced by the HET-PHIP approach used hyperpolarized propane produced over immobilized catalysts [53, 54]; further work extended these studies to the MR imaging of propane produced over supported metal catalysts [55]. Despite the limitations associated with a relatively short nuclear spin relaxation time that characterizes the lifetime of the enhanced NMR signals, hyperpolarized propane can be successfully used to obtain images with relatively high spatial resolution. The lifetime of propane hyperpolarization is substantially longer in low magnetic fields [56, 57], which is advantageous for low-field MRI studies [58]. Rh/TiO_2 catalyst is currently the most efficient one in producing hyperpolarized propane for MRI experiments. It was found that the maximum signal gain is observed for the low propylene fraction (~10%) in the propylene-parahydrogen mixture at low or intermediate total gas pressure (1–3 atm). The latter result is consistent with

previous studies in which, upon hydrogenation of propylene on Pt/Al_2O_2 catalysts, an approximately linear increase in the PHIP effect was observed with the increase in partial pressure of parahydrogen [59].

The very first visualization of catalytic processes in an operating model reactor using HET-PHIP was based on hydrogenation of propylene with p-H_2 in a piece of tubing with 1/8'' o.d. packed with either a granular bed of Wilkinson's catalyst immobilized on silica support, or simply powdered Wilkinson's catalyst [53]. A mixture of propylene and p-H_2 flowed through the reactor that was residing in the probe of a microimaging instrument and maintained at 145 °C. The signal of propane gas in the void space of the catalyst bed demonstrated enhancement factor of ca. 300. This allowed the authors to map the distribution of the hyperpolarized propane gas inside the operating reactor; at the same time, no meaningful images could be detected when using thermally polarized gas.

The experiments were later extended to MRI of microfluidic chips [60] and microreactors [61] by combining HET-PHIP with the so-called remote detection (RD) NMR [62–64]. In RD NMR, the image encoding and detection are separated in space. A reactor or a microfluidic chip is residing in the encoding rf coil which manipulates nuclear spin magnetization of a fluid within the reactor to encode spatial information, but NMR signal acquisition is performed with a separate rf microcoil downstream of the reactor as the fluid flows out of the reactor and into the detection coil. In addition to spatial information on the position of the fluid elements within the reactor at the moment of encoding, this experiment also yields the time-of-flight information. The optimized size of the detection microcoil endows RD NMR with significant signal enhancement even without the use of nuclear spin hyperpolarization.

HET-PHIP and RD NMR were previously combined to monitor propylene hydrogenation over Rh/SiO_2 and Rh/TiO_2 catalysts [61]. The combined sensitivity gain provided by PHIP and RD NMR detection scheme was ca. 5×10^4-fold. This made it possible to quantify the distribution of hyperpolarized propane within the packed-bed microreactors with diameters from 800 down to 150 μm. The TOF data were used to evaluate gas flow velocities within the catalyst bed and kinetic parameters of the reaction. In addition, this experimental approach made it possible to quantify gas adsorption under reactive and non-reactive conditions [65]. Because of the availability of the full spectral information in the NMR spectra, TOF images for the individual gases can be produced, allowing one to study competitive adsorption of different gases.

The heterogeneous nature of a granular catalyst bed causes significant complications for the MRI experiments by distorting the applied magnetic field of the imaging instrument. This drastically degrades the spectral resolution and causes artifacts in the MR images. To overcome this problem, MRI-compatible model glass reactors with catalytically active coatings deposited on their walls were developed and implemented in the operando MRI studies of heterogeneous hydrogenations with parahydrogen [66, 67]. In particular, MRI was applied to visualize catalytic hydrogenation of propylene using Rh nanoparticles supported on a TiO_2 layer deposited on the glass tubular reactors [66]. These coatings on the reactor walls were catalytically active in the hydrogenation of propylene at room temperature, leading to the formation of enhanced ^{1}H NMR propane signals due to the pairwise addition of molecular hydrogen to the substrate. It is noteworthy that the productivity of the fabricated catalytic reactors was stable even after 9 days of use, with the observed signal enhancement reduced only 3-fold over this time period. The set of acquired 2D images was used to perform 3D rendering of the operating model reactor. In the later study [67], the NMR spectra of the reacting mixture were acquired with the spatial resolution along the reactor axis, providing the spatial information within the reactor on the catalytic conversion (Fig. 12).

The hyperpolarization methods are currently being pushed toward *in vivo* MRI and MRS studies of lab animals and even humans [68]. The approach has a tremendous potential for revealing the abnormalities of cell metabolism, paving the way toward an advanced medical tool for diagnostics of cancer and many other pathologies and diseases at a very early stage. A prerequisite for such applications is the development of techniques for hyperpolarizing biologically relevant endogenous and exogenous substances, a significant prolongation of the hyperpolarization lifetime from seconds to tens of seconds and more, and the use of aqueous media for administering hyperpolarized substances in a living organism by an injection. Transfer of polarization from ^{1}H to other nuclei such as ^{13}C and ^{15}N is a well-established approach for extending the lifetime of hyperpolarized spin states in magnetic resonance. To this end, hydrogenation of vinyl acetate

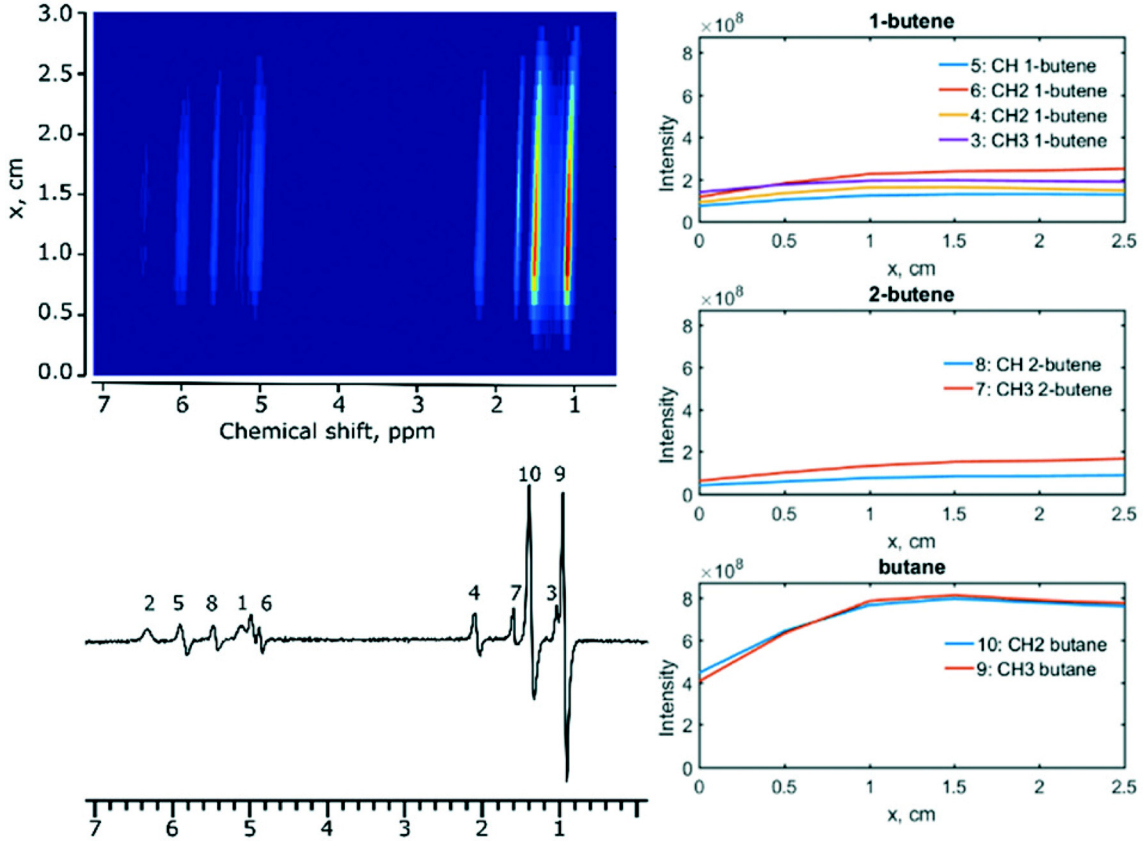

Fig. 12: Hydrogenation of 1,3-butadiene with p-H_2 over Ir/SiO_2 catalyst as followed by combining NMR spectroscopy with MRI. The reaction was performed at 130 °C using 1,3-butadiene: p-H_2 = 1 : 4 mixture supplied at the 5.1 ml/s flow rate. Top panel: distribution of the intensities of NMR signals in the working reactor along its axis. Bottom panel: ^{1}H NMR spectrum obtained in a PASADENA experiment. Right panels: plots of the distribution of the reaction products along the length of the reactor. Reproduced from [67] with permission from The Royal Society of Chemistry.

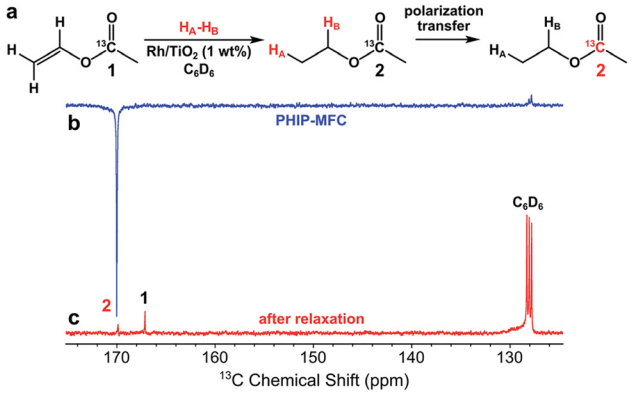

Fig. 13: a) Reaction scheme for heterogeneous hydrogenation of vinyl acetate-1–^{13}C with p-H_2 over 1 wt.% Rh/TiO_2 catalyst in benzene-d6 solution, with subsequent polarization transfer from ^{1}H to ^{13}C nuclei via magnetic field cycling. b) ^{13}C NMR spectrum of hyperpolarized ethyl[1–^{13}C]acetate, and c) the corresponding spectrum of thermally polarized reaction mixture after relaxation of nuclear spins to thermal equilibrium. Reproduced from [70] with permission from The Royal Society of Chemistry.

with parahydrogen over a Rh/TiO_2 catalyst [69–71] was implemented both in the liquid and gas phases, producing ethyl acetate with a relatively strong hyperpolarization of ^{1}H nuclei. Polarization transfer from ^{1}H to ^{13}C nuclei in ethyl acetate (Fig. 13) as well as its hydrolysis in aqueous medium to produce ethanol and acetate with the partial retention of hyperpolarization [70] were successfully demonstrated, providing the necessary step toward future biomedical applications of this approach. The utilization of heterogeneous

catalysts in such processes is essential because homogeneous metal complexes are very difficult to remove rapidly and completely from the reaction medium after reaction is completed to produce a biocompatible injectable solution of a hyperpolarized metabolite. Large scale batch mode production of hyperpolarized propane has been also demonstrated [72], which has certain potential for future biomedical lung imaging applications.

Conclusions

The use of parahydrogen in catalytic reactions can enhance NMR signals of the reaction products and intermediates by as much as 1000-fold and even more due to the phenomenon of parahydrogen-induced polarization (PHIP) of nuclear spins. It is remarkable, and possibly still somewhat surprising, that this can be achieved not only in homogeneous hydrogenations, but also in heterogeneous catalytic processes that involve H_2 as one of the key reactants. Furthermore, the efforts of the preceding 10–15 years have revealed that PHIP effects in heterogeneous hydrogenations (HET-PHIP) is not an exception but in fact is a rather general phenomenon observable with many different types of heterogeneous catalysts, including immobilized metal complexes, supported metal nanoparticles, bulk and supported metal oxides, sulfides and carbides, as well as single metal atom and single-atom alloy catalysts [24, 73]. This fact is an important prerequisite for developing a useful hypersensitive NMR-based tool for advanced mechanistic studies in heterogeneous catalysis. In addition, the utilization of heterogeneous catalysts for the production of highly polarized molecules is of interest in its own right as it is very promising for the development of advanced MRI techniques for the studies in chemistry, materials science, and biomedicine. While a lot has been already achieved, as illustrated with the examples provided above, there is little doubt that this is just a beginning of a long and productive journey toward novel scientific and practical developments. In particular, extension of the PHIP approach to metal-free systems such as amine-borane frustrated Lewis pairs (FLP) in solution has been already demonstrated [74], and there is probably no reason why this approach cannot be extended to address surface FLP. A major progress can be potentially achieved in yet another direction, namely the extension of this approach to catalytic processes that do not use H_2. The feasibility of such an extension is based on the fact that symmetric gaseous molecules other than H_2 also have different nuclear spin modifications, called nuclear spin isomers, which are analogous to ortho- and parahydrogen. Spin isomers of methane, formaldehyde, ethylene, ammonia, etc., can be used to boost NMR sensitivity, thus providing very important mechanistic information about a range of very important industrial catalytic transformations. At present, enriched spin isomers of molecules other than H_2 and D_2 are not readily available, but the work in this direction has already demonstrated certain achievements. In particular, catalytic enrichment of spin isomers of ethylene [75] is another promising area where catalysis and magnetic resonance can have a mutually beneficial cooperation.

Funding: The authors thank the Russian Foundation for Basic Research (Grants 17-54-33037, 19-53-12013, 19-29-10003) and the Russian Ministry of Science and Higher Education (AAAA-A16-116121510087-5) for financial support. O.G.S. thanks the Russian Foundation for Basic Research (Grant 19-33-60045) for the support of mechanistic studies of heterogeneous hydrogenations with the use of parahydrogen.

References

[1] V. V. Zhivonitko, I. V. Skovpin, K. C. Szeto, M. Taoufik, I. V. Koptyug. *J. Phys. Chem. C* **122**, 4891 (2018).
[2] C. R. Bowers, D. P. Weitekamp. *J. Am. Chem. Soc.* **109**, 5541 (1987).
[3] S. B. Duckett, N. J. Wood. *Coord. Chem. Rev.* **252**, 2278 (2008).
[4] P. Jurt, O. Salnikov, T. L. Gianetti, N. Chukanov, M. G. Baker, G. Le Corre, J. E. Borger, R. Verel, S. Gauthier, O. Fuhr, K. V. Kovtunov, A. Fedorov, D. Fenske, I. V. Koptyug, H. Grutzmacher. *Chem. Sci.* **10**, 7937 (2019).

[5] I. V. Koptyug, K. V. Kovtunov, S. R. Burt, M. S. Anwar, C. Hilty, S. Han, A. Pines, R. Z. Sagdeev. *J. Am. Chem. Soc.* **129**, 5580 (2007).
[6] K. V. Kovtunov, I. V. Koptyug. In *Magnetic Resonance Microscopy: Spatially Resolved NMR Techniques and Applications*, S. Codd, J. D. Seymour (Eds.) pp. 101–115. Wiley-VCH, Weinheim (2008).
[7] C. Jones. *Topics in Catalysis* **53**, 942 (2010).
[8] I. V. Skovpin, V. V. Zhivonitko, I. V. Koptyug. *Appl. Magn. Reson.* **41**, 393 (2011).
[9] T. Gutmann, T. Ratajczyk, Y. Xu, H. Breitzke, A. Grunberg, S. Dillenberger, U. Bommerich, T. Trantzschel, J. Bernarding, G. Buntkowsky. *Solid State NMR* **38**, 90 (2010).
[10] S. Abdulhussain, H. Breitzke, T. Ratajczyk, A. Grunberg, M. Srour, D. Arnaut, H. Weidler, U. Kunz, H. J. Kleebe, U. Bommerich, J. Bernarding, T. Gutmann, G. Buntkowsky. *Chem. Eur. J.* **20**, 1159 (2014).
[11] I. V. Skovpin, V. V. Zhivonitko, R. Kaptein, I. V. Koptyug. *Appl. Magn. Reson.* **44**, 289 (2013).
[12] I. V. Skovpin, V. V. Zhivonitko, I. P. Prosvirin, D. F. Khabibulin, I. V. Koptyug. *Z. Phys. Chem.* **231**, 575 (2016).
[13] K. V. Kovtunov, V. V. Zhivonitko, A. Corma, I. V. Koptyug. J. Phys. *Chem. Lett.* **1**, 1705 (2010).
[14] Q. Gong, J. Klankermayer, B. Blumich. *Chem. Eur. J.* **17**, 13795 (2011).
[15] E. d. V. Gomez, S. Amaya-Roncancio, L. B. Avalle, D. H. Linares, M. C. Gimenez. *Appl. Surf, Sci.* **420**, 1 (2017).
[16] K. V. Kovtunov, I. E. Beck, V. I. Bukhtiyarov, I. V. Koptyug. *Angew. Chem. Int. Ed.* **47**, 1492 (2008).
[17] K. V. Kovtunov, I. E. Beck, V. V. Zhivonitko, D. A. Barskiy, V. I. Bukhtiyarov, I. V. Koptyug. *Phys. Chem. Chem. Phys.* **14**, 11008 (2012).
[18] O. G. Salnikov, D. B. Burueva, E. Y. Gerasimov, A. V. Bukhtiyarov, A. K. Khudorozhkov, I. P. Prosvirin, L. M. Kovtunova, D. A. Barskiy, V. I. Bukhtiyarov, K. V. Kovtunov, I. V. Koptyug. *Catal. Today* **283**, 82 (2017).
[19] E. Pokochueva, K. V. Kovtunov, O. Salnikov, M. Gemeinhardt, L. Kovtunova, V. Bukhtiyarov, B. M. Goodson, E. Chekmenev, I. V. Koptyug. *Phys. Chem. Chem. Phys.* **21**, 26477 (2019).
[20] V. V. Zhivonitko, K. V. Kovtunov, I. E. Beck, A. B. Ayupov, V. I. Bukhtiyarov, I. V. Koptyug. *J. Phys. Chem. C* **115**, 13386 (2011).
[21] V. V. Zhivonitko, I. V. Skovpin, M. Crespo-Quesada, L. Kiwi-Minsker, I. V. Koptyug. *J. Phys. Chem. C* **120**, 4945 (2016).
[22] D. A. Barskiy, K. V. Kovtunov, A. Primo, A. Corma, R. Kaptein, I. V. Koptyug. *ChemCatChem* **4**, 2031 (2012).
[23] K. V. Kovtunov, D. A. Barskiy, O. G. Salnikov, D. B. Burueva, A. K. Khudorozhkov, A. V. Bukhtiyarov, I. P. Prosvirin, E. Y. Gerasimov, V. I. Bukhtiyarov, I. V. Koptyug. *ChemCatChem* **7**, 2581 (2015).
[24] K. V. Kovtunov, V. V. Zhivonitko, I. V. Skovpin, D. A. Barskiy, I. V. Koptyug. *Top. Curr. Chem.* **338**, 123 (2013).
[25] O. G. Salnikov, D. A. Barskiy, D. B. Burueva, Y. K. Gulyaeva, B. S. Balzhinimaev, K. V. Kovtunov, I. V. Koptyug. *Appl. Magn. Reson.* **45**, 1051 (2014).
[26] I. V. Koptyug, V. V. Zhivonitko, K. V. Kovtunov. *ChemPhysChem* **11**, 3086 (2010).
[27] O. G. Salnikov, L. M. Kovtunova, I. V. Skovpin, V. I. Bukhtiyarov, K. V. Kovtunov, I. V. Koptyug. *ChemCatChem* **10**, 1178 (2018).
[28] D. B. Burueva, O. G. Salnikov, K. V. Kovtunov, A. S. Romanov, L. M. Kovtunova, A. K. Khudorozhkov, A. V. Bukhtiyarov, I. P. Prosvirin, V. I. Bukhtiyarov, I. V. Koptyug. *J. Phys. Chem. C* **120**, 13541 (2016).
[29] O. Salnikov, K. Kovtunov, P. Nikolaou, L. Kovtunova, V. I. Bukhtiyarov, I. V. Koptyug, E. Y. Chekmenev. *ChemPhysChem* **19**, 2621 (2018).
[30] O. G. Salnikov, H.-J. Liu, A. Fedorov, D. Burueva, K. V. Kovtunov, C. Coperet, I. V. Koptyug. *Chem. Sci.* **8**, 2426 (2017).
[31] K. V. Kovtunov, V. V. Zhivonitko, I. V. Skovpin, O. G. Salnikov, I. V. Koptyug. In *Magnetic nanomaterials: applications in catalysis and life sciences*, S. H. Bossmann, H. Wang (Eds.), pp. 142–171, The Royal Society of Chemistry (2017).
[32] H.-H. Limbach, G. Buntkowsky, J. Matthes, S. Grundemann, T. Pery, B. Walaszek, *B. Chaudret. ChemPhysChem* **7**, 551 (2006).
[33] E. Ilisca. *Progr. Surf. Sci.* **41**, 217–335 (1992).
[34] R. Sharma, L. S. Bouchard. *Sci. Rep.* **2**, 277 (2012).
[35] J. McCormick, A. M. Grunfeld, Y. N. Ertas, A. N. Biswas, K. L. Marsh, S. Wagner, S. Gloggler, L.-S. Bouchard. *Anal. Chem.* **89**, 7190 (2017).
[36] A. Corma, O. G. Salnikov, D. A. Barskiy, K. V. Kovtunov, I. V. Koptyug. *Chem. Eur. J.* **21**, 7012 (2015).
[37] R. Lin, D. Albani, E. Fako, S. K. Kaiser, O. V. Safonova, N. Lopez, J. Perez-Ramirez. *Angew. Chem. Int. Ed.* **58**, 504 (2019).
[38] D. P. Estes, G. Siddiqi, F. Allouche, K. V. Kovtunov, O. E. Safonova, A. L. Trigub, I. V. Koptyug, C. Coperet. *J. Am. Chem. Soc.* **138**, 14987 (2016).
[39] M. F. Delley, M.-C. Silaghi, F. Nunez-Zarur, K. V. Kovtunov, O. G. Salnikov, D. P. Estes, I. V. Koptyug, A. Comas-Vives, C. Coperet. Organomet. **36**, 234 (2017).
[40] G. Vile, D. Albani, M. Nachtegaal, Z. Chen, D. Dontsova, M. Antonietti, N. Lopez, J. Perez-Ramirez. *Angew. Chem. Int. Ed.* **54**, 11265 (2015).
[41] Z. Chen, S. Mitchell, E. Vorobyeva, R. K. Leary, R. Hauert, T. Furnival, Q. M. Ramasse, J. M. Thomas, P. A. Midgley, D. Dontsova, M. Antonietti, S. Pogodin, N. Lopez, J. Perez-Ramirez. *Adv. Funct. Mater.* **27**, 1605785 (2017).
[42] F. Huang, Y. Deng, Y. Chen, X. Cai, M. Peng, Z. Jia, P. Ren, D. Xiao, X. Wen, N. Wang, H. Liu, D. Ma. *J. Am. Chem. Soc.* **140**, 13142 (2018).
[43] D. B. Burueva, K. V. Kovtunov, A. V. Bukhtiyarov, D. A. Barskiy, I. P. Prosvirin, I. S. Mashkovsky, G. N. Baeva, V. I. Bukhtiyarov, A. Y. Stakheev, I. V. Koptyug. *Chem. Eur. J.* **24**, 2547 (2018).

[44] K. V. Kovtunov, D. A. Barskiy, O. G. Salnikov, A. K. Khudorozhkov, V. I. Bukhtiyarov, I. P. Prosvirin, I. V. Koptyug. *Chem. Commun.* **50**, 875 (2014).
[45] E. W. Zhao, H. Zheng, R. Zhou, H. E. Hagelin-Weaver, C. R. Bowers. *Angew. Chem. Int. Ed.* **54**, 14270 (2015).
[46] E. W. Zhao, Y. Xin, H. E. Hagelin-Weaver, C. R. Bowers. *ChemCatChem* **8**, 2197 (2016).
[47] O. G. Salnikov, D. B. Burueva, D. A. Barskiy, G. A. Bukhtiyarova, K. V. Kovtunov, I. V. Koptyug. *ChemCatChem* **7**, 3508 (2015).
[48] D. B. Burueva, A. A. Smirnov, O. A. Bulavchenko, I. P. Prosvirin, E. Y. Gerasimov, V. A. Yakovlev, K. V. Kovtunov, I. V. Koptyug. *Topics in Catalysis* **63**, 2 (2020).
[49] V. V. Zhivonitko, A. I. Svyatova, K. V. Kovtunov, I. V. Koptyug. *Annu. Rep. NMR Spectrosc.* **95**, 83 (2018).
[50] A. I. Svyatova, K. V. Kovtunov, I. V. Koptyug. *Rev. Chem. Eng.* (2019); https://doi.org/10.1515/revce-2018-0035.
[51] A. A. Lysova, I. V. Koptyug. *Chem. Soc. Rev.* **39**, 4585 (2010).
[52] I. V. Koptyug. In *Spectroscopic Properties of Inorganic and Organometallic Compounds*, R. Douthwaite, S. Duckett, J. Yarwood, (Eds.), pp. 1–42, Royal Society of Chemistry, Cambridge (2014).
[53] L.-S. Bouchard, S. R. Burt, M. S. Anwar, K. V. Kovtunov, I. V. Koptyug, A. Pines. *Science* **319**, 442 (2008).
[54] L.-S. Bouchard, K. V. Kovtunov, S. R. Burt, M. S. Anwar, I. V. Koptyug, R. Z. Sagdeev, A. Pines. *Angew. Chem. Int. Ed.* **46**, 4064 (2007).
[55] K. V. Kovtunov, D. A. Barskiy, A. M. Coffey, M. L. Truong, O. G. Salnikov, A. K. Khudorozhkov, E. A. Inozemtseva, I. P. Prosvirin, V. I. Bukhtiyarov, K. W. Waddell, E. Y. Chekmenev, I. V. Koptyug. *Chem. Eur. J.* **20**, 11636 (2014).
[56] K. V. Kovtunov, M. L. Truong, D. A. Barskiy, I. V. Koptyug, A. M. Coffey, K. W. Waddell, E. Y. Chekmenev. *Chem. Eur. J.* **20**, 14629 (2014).
[57] N. M. Ariyasingha, O. G. Salnikov, K. V. Kovtunov, L. M. Kovtunova, V. I. Bukhtiyarov, B. M. Goodson, M. S. Rosen, I. V. Koptyug, J. G. Gelovani, E. Y. Chekmenev. *J. Phys. Chem. C* **123**, 11734 (2019).
[58] K. V. Kovtunov, M. L. Truong, D. A. Barskiy, O. G. Salnikov, V. I. Bukhtiyarov, A. M. Coffey, K. W. Waddell, I. V. Koptyug, E. Y. Chekmenev. *J. Phys. Chem. C* **118**, 28234 (2014).
[59] O. G. Salnikov, K. V. Kovtunov, D. A. Barskiy, V. I. Bukhtiyarov, R. Kaptein, I. V. Koptyug. *Appl. Magn. Reson.* **44**, 279 (2013).
[60] V.-V. Telkki, V. V. Zhivonitko, S. Ahola, K. V. Kovtunov, J. Jokisaari, I. V. Koptyug. *Angew. Chem. Int. Ed.* **49**, 8363 (2010).
[61] V. V. Zhivonitko, V.-V. Telkki, I. V. Koptyug. *Angew. Chem. Int. Ed.* **51**, 8054 (2012).
[62] E. E. McDonnell, S.-I. Han, C. Hilty, K. L. Pierce, A. Pines. *Anal. Chem.* **77**, 8109 (2005).
[63] M. S. Anwar, C. Hilty, C. Chu, L.-S. Bouchard, K. Pierce, A. Pines. *Anal. Chem.* **79**, 2806 (2007).
[64] V.-V. Telkki, V. V. Zhivonitko. *J. Magn. Reson.* **210**, 238 (2011).
[65] A. Selent, V. V. Zhivonitko, I. V. Koptyug, V.-V. Telkki. *Microporous Mesoporous Mater.* **269**, 148 (2018).
[66] K. V. Kovtunov, D. Lebedev, A. Svyatova, E. V. Pokochueva, I. P. Prosvirin, E. Y. Gerasimov, V. I. Bukhtiyarov, C. R. Muller, A. Fedorov, I. V. Koptyug. *ChemCatChem* **11**, 969 (2019).
[67] A. Svyatova, E. S. Kononenko, K. V. Kovtunov, D. Lebedev, E. Y. Gerasimov, A. Bukhtiyarov, I. Prosvirin, V. Bukhtiyarov, C. R. Muller, A. Fedorov, I. V. Koptyug. *Catal. Sci. Technol.* **10**, 99 (2020).
[68] J. Kurhanewicz, D. B. Vigneron, J. H. Ardenkjaer-Larsen, J. A. Bankson, K. Brindle, C. H. Cunningham, F. A. Gallagher, K. R. Keshari, A. Kjaer, C. Laustsen, D. A. Mankoff, M. E. Merritt, S. J. Nelson, J. M. Pauly, P. Lee, S. Ronen, D. J. Tyler, S. S. Rajan, D. M. Spielman, L. Wald, X. Zhang, C. R. Malloy, R. Rizi. *Neoplasia* **21**, 1 (2019).
[69] O. G. Salnikov, K. V. Kovtunov, I. V. Koptyug. *Sci. Rep.* **5**, 13930 (2015).
[70] K. V. Kovtunov, D. A. Barskiy, O. G. Salnikov, R. V. Shchepin, A. M. Coffey, L. M. Kovtunova, V. I. Bukhtiyarov, I. V. Koptyug, E. Chekmenev. *RSC Adv.* **6**, 69728 (2016).
[71] K. V. Kovtunov, D. A. Barskiy, R. V. Shchepin, O. G. Salnikov, I. P. Prosvirin, A. V. Bukhtiyarov, L. M. Kovtunova, V. I. Bukhtiyarov, I. V. Koptyug, E. Y. Chekmenev. *Chem. Eur. J.* **22**, 16446 (2016).
[72] O. G. Salnikov, P. Nikolaou, N. M. Ariyasingha, K. V. Kovtunov, I. V. Koptyug, E. Y. Chekmenev. *Anal. Chem.* **91**, 4741 (2019).
[73] K. V. Kovtunov, O. G. Salnikov, V. V. Zhivonitko, I. V. Skovpin, V. I. Bukhtiyarov, I. V. Koptyug. *Topics in Catalysis* **59**, 1686 (2016).
[74] V. V. Zhivonitko, K. Sorochkina, K. Chernichenko, B. Kotai, T. Foldes, I. Papai, V.-V. Telkki, T. Repo, I. Koptyug. *Phys. Chem. Chem. Phys.* **18**, 27784 (2016).
[75] V. V. Zhivonitko, K. V. Kovtunov, P. L. Chapovsky, I. V. Koptyug. *Angew. Chem. Int. Ed.* **52**, 13251 (2013).